THE JOURNAL OF BIOLOGICAL CHEMISTRY
Vol. 279, No. 27, Issue of July 2, pp. 28435–28442, 2004
Printed in U.S.A.

Preferential Substrate Binding Orientation by the Molecular Chaperone HscA*[S]

Received for publication, January 25, 2004, and in revised form, April 16, 2004
Published, JBC Papers in Press, April 20, 2004, DOI 10.1074/jbc.M400803200

Tim L. Tapley and Larry E. Vickery‡

From the Department of Physiology and Biophysics, University of California, Irvine, California 92697

HscA, a specialized bacterial hsp70-class chaperone, interacts with the iron-sulfur cluster assembly protein IscU by recognizing a conserved LPPVK sequence motif at positions 99–103. We have used a site-directed fluorescence labeling and quenching strategy to determine whether HscA binds to IscU in a preferred orientation. HscA was selectively labeled on opposite sides of the substrate binding domain with the fluorescent probe bimane, and the ability of LPPVK-containing peptides having tryptophan at the N or C terminus to quench bimane fluorescence was measured. Quenching was highly dependent on the position of tryptophan in the peptide and the location of bimane on HscA implying a strong directional preference for peptide binding. Similar experiments showed that full-length IscU binds in the same orientation as IscU-derived peptides and that binding orientation is unaffected by the co-chaperone HscB. The preferred orientation of the HscA-IscU complex is the reverse of that previously described for peptide complexes of *Escherichia coli* DnaK and rat Hsc70 substrate binding domain fragments establishing that hsp70 isoforms can bind peptide/polypeptide substrates in different orientations.

HscA is an hsp70 class molecular chaperone (M_r 66,000; also designated Hsc66) that is constitutively expressed in *Escherichia coli* (1–3). Genetic studies in bacteria and eukaryotes indicate that HscA participates in the biogenesis of iron-sulfur proteins (4–7). The exact role of HscA is not known, but HscA binds IscU (8, 9), a protein proposed to serve as a template for iron-sulfur cluster formation (10, 11), and may function to regulate cluster formation on IscU or transfer of iron-sulfur clusters from IscU to acceptor proteins. The interaction between HscA and IscU is facilitated by HscB (also designated Hsc20), a J-type co-chaperone protein that binds both IscU and HscA and targets IscU to HscA (3, 8, 9).

Recently, we found that HscA specifically recognizes a conserved LPPVK sequence motif found at positions 99–103 of IscU (12). A synthetic peptide corresponding to residues 98–106 (ELPPVKIHC) was found to bind to HscA and to stimulate HscA ATPase activity in a manner similar to IscU, suggesting that the LPPVK region plays a key role in binding to and regulation of HscA. Amino acid replacement studies on IscU and the Glu^{98}–Cys^{106} peptide[1] revealed that Pro^{101} is the most critical position with Val^{102} and Lys^{103} also contributing to high affinity binding and regulation (13). To better understand the interaction of IscU with HscA we used the crystal structure of DnaK bound to the synthetic peptide NRLLLTG (14) to construct models of HscA-peptide complexes (13). These models suggested that the LPPVK region of IscU could be accommodated in the peptide binding cleft of the substrate binding domain of HscA with the peptide backbone in an extended conformation, and the importance of Pro^{101} could be rationalized by its projection into a hydrophobic pocket in the central position of the cleft. It was not possible, however, to determine the orientation of the peptide based on model analysis, only minor differences in HscA or peptide structure were observed in models in which the peptide was oriented in opposite directions relative to the substrate binding domain (13). Furthermore, interactions of HscA with other regions of the IscU protein or with the co-chaperone HscB could impose steric constraints on binding and dictate orientation of the peptide in the complex.

In the studies described herein, we have employed site-directed fluorescence labeling and quenching to determine whether HscA binds to IscU-based peptides and the full-length IscU protein in a specific orientation. The results suggest that HscA has a strong directional preference for substrate binding and that the preferred orientation is opposite that previously reported for peptide complexes of other hsp70 proteins.

EXPERIMENTAL PROCEDURES

Site-directed Mutagenesis, Protein Expression, and Purification—Site-directed mutants of HscA and IscU were constructed using the QuikChange technique (Stratagene) with oligonucleotides from Integrated DNA Technologies, Inc. Mutations were confirmed by DNA sequencing (Laragen, Inc). The plasmid pTrcHscA(C315S/C448S) was constructed from pTrcHscA (3) by mutation of codons for residues Cys^{315} and Cys^{448} to encode serine. This plasmid was used as a template to construct the HscA(Q421C), HscA(D422C), and HscA(A455C) mutants such that each would have a single cysteine codon. pTrcIscU (8) was used as a template for the IscU(L97W) and IscU(H105W) mutants. Expression and purification of HscA and IscU mutants were carried out as previously described for the wild-type proteins (3, 8).

Synthetic Peptides—Glu^{98}–Cys^{106}, W-97, and W-105 (*cf.* Fig. 1) were synthesized by the Protein and Nucleic Acid Biotechnology facility at Stanford University. Peptides were purified by high pressure liquid chromatography, and composition was confirmed by mass spectrometry. Concentrations of Glu^{98}–Cys^{106} were determined using Ellman's reagent (15), and concentrations of W-97 and W-105 were determined assuming ϵ_{280} = 5,600 M^{-1} cm^{-1} for tryptophan (16–18).

Bimane Labeling—HscA(Q421C), HscA(D422C), and HscA(A455C) were treated with a 10-fold molar excess of monobromobimane (Molec-

* This work was supported by National Institutes of Health Grants GM54264 (to L. E. V.) and NCI Carcinogenesis Training Program Grant 5T32CA09054 (to T. L. T.). The costs of publication of this article were defrayed in part by the payment of page charges. This article must therefore be hereby marked "*advertisement*" in accordance with 18 U.S.C. Section 1734 solely to indicate this fact.

[S] The on-line version of this article (available at http://www.jbc.org) contains supplemental Figs. 1 and 2.

‡ To whom correspondence should be addressed. Tel.: 949-824-6580; Fax: 949-824-8540; E-mail: lvickery@uci.edu.

[1] The abbreviations used are: Glu^{98}–Cys^{106} peptide, ELPPVKIHC peptide corresponding to IscU residues 98–106; HscA(Q421C)-bimane, HscA(D422C)-bimane, and HscA(A455C)-bimane, bimane-labeled HscA triple mutants derived from HscA(C315S/C448S); W-97 peptide, WELPPVKI; W-105 peptide, ELPPVKIW.

ular Probes) in 10 mM Tris, 1 mM EDTA, pH 8.0, for 30 min at 25 °C and then overnight at 4 °C, and excess label was removed using G-25 spin columns (Amersham Biosciences). Labeling was assessed spectrophotometrically using the following extinction coefficients: HscA ϵ_{280} = 19,600 M^{-1} cm^{-1} (3); bimane ϵ_{280} = 3,600 M^{-1} cm^{-1}, ϵ_{380} = 5,000 M^{-1} cm^{-1} (19). The cysteine-free mutant, HscA(C315S/C448S), gave a labeling stoichiometry <0.1:1 indicating a low level of nonspecific label incorporation. The HscA(Q421C), HscA(D422C), and HscA(A455C) mutants gave labeling stoichiometries ≅1:1 (range 0.65–1.1:1 in different experiments) consistent with specific labeling of the single cysteine residue present.

Fluorescence Measurements—Fluorescence spectra were recorded using a SLM 8100 steady-state fluorescence spectrometer (Jobin Yvon). All measurements were recorded at 25 °C using a 4 × 10-mm cuvette. Samples contained bimane-labeled HscA (1–2 μM) in HKM buffer (50 mM HEPES, 150 mM KCl, 10 mM $MgCl_2$, pH 7.5). For experiments in the presence of ADP (1 mM) samples were preincubated 30 min to allow hydrolysis of small amounts of contaminating ATP. For experiments in the presence of ATP (5 mM) the slow intrinsic rate of hydrolysis was estimated to reduce ATP concentrations <2% during the time required for measurements. Corrected emission spectra (4-nm band pass) were recorded from 420 to 520 nm at 1-nm intervals using an excitation wavelength of 395 nm (8-nm band pass) and a scan rate of 1 nm/s. Spectral scans were repeated to test for time-dependent effects, and all samples were found to exhibit rapid equilibration. Peptide titrations were carried out by stepwise additions (1.5–130 μl) from 0.6, 3.0, or 5.7 mM stock solutions in HKM buffer. IscU titrations were carried out by stepwise additions (2.5–60 μl) of 1 mM stock solutions in HKM buffer. For experiments in the presence of HscB, emission spectra of bimane-labeled HscA were recorded in the presence of 5 mM ATP before and after the addition of a pre-equilibrated solution of HscB and IscU (each 57 μM final concentration) in HKM buffer. Emission data were integrated by taking the sum of emission intensities from 420 to 520 nm. Spectral titrations were carried out 2–4 times with similar results, and representative data from individual experiments are shown in Figs. 3–8.

Other Methods—ATPase assays, isothermal titration calorimetry, and rhodanese aggregation studies were carried out as described previously (3, 20, 21). ATPase activities given in Table I are the average of three determinations; standard deviation values ranged from ±0.8% for rates >40 min^{-1} to ±5.3% for rates ~0.1 min^{-1}. Correction and integration of emission spectra were carried out using Excel (Microsoft), and curve fitting was performed using KaleidaGraph (Synergy Software).

RESULTS

Experimental Rationale—We used site-directed labeling with the fluorescent probe bimane and quenching by tryptophan containing peptides (see Fig. 1) to determine the orientation of substrates bound to HscA. This approach takes advantage of the short-range quenching of bimane fluorescence by tryptophan, a process that involves collisional contact between the bimane excited state and the indole ring of tryptophan (22, 23). Bimane fluorescence displays some variation with environmental parameters (19, 24), but its efficient quenching by tryptophan can provide a measure of short-range interactions in proteins (25). The substrate binding domain of HscA was selectively labeled with monobromobimane, and the ability of IscU-derived peptides having tryptophan at the N or C terminus (W-97 and W-105) to quench bimane fluorescence was measured. Mutant forms of the full-length IscU protein having tryptophan in the corresponding positions (L97W and H105W) were also tested for their ability to quench bimane-labeled HscA.

We have recently constructed models of the substrate binding domain of HscA bound to the IscU peptide ELPPVKI (13) based on the crystal structure of the DnaK substrate binding domain complexed to the peptide NRLLLTG (14). The β-sandwich subdomain of HscA exhibits 50% sequence identity to that of DnaK, suggesting that the peptide binding regions are likely to have similar structures. Fig. 2 shows different views of a model of the HscA substrate binding domain complexed with peptide. The peptide is located in a groove in the β-sandwich subdomain with Pro^{101} projecting downward into a hydrophobic pocket in the central region of the cleft. In this model the peptide is positioned with the N terminus (Glu^{98}) located on the

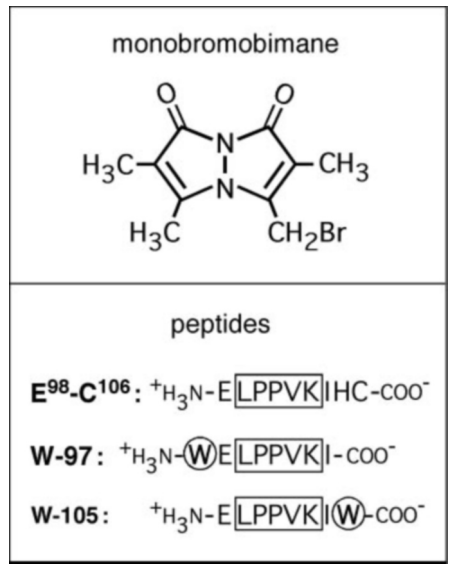

FIG. 1. **Structures of the fluorescent label bimane and IscU-derived peptides.** The structure of monobromobimane used for cysteine labeling is shown. For peptides, the amino acid sequence of IscU recognized by HscA (12) is *boxed*, and N- and C-terminal tryptophan residues added to quench bimane fluorescence are *circled*.

"back" side of the substrate binding domain and the C terminus (Ile^{104}) located on the "front" side. This orientation is opposite that observed for the DnaK-NRLLLTG peptide complex (14). We have designated the back to front orientation shown as the "reverse" direction relative to the "forward" direction originally observed for the DnaK-NRLLLTG peptide complex. To identify positions for bimane labeling we inspected the model for surface residues close to the position at which the peptide exits the binding cleft. Gln^{421} and Asp^{422}, located just below the cleft on the front side, and Ala^{455}, located just below the cleft on the back side, appeared to provide labeling sites that might allow bimane to selectively interact with N- or C-terminal residues of bound peptides.

Cysteine Mutants of HscA—Cysteine residues were introduced into HscA at positions 421, 422, or 455 to allow bimane labeling. To ensure specific labeling at these sites the endogenous cysteine residues at positions 315 and 448 of HscA were first changed to serine by mutagenesis. This resulting double mutant, HscA(C315S/C448S), was then used as a template to generate three triple mutants, designated HscA(Q421C), HscA(D422C), and HscA(A455C), containing unique cysteine labeling sites. Each of the mutants behaved similarly to wild-type HscA during purification, suggesting that no gross structural changes resulted from the amino acid replacements.

To assess whether the different cysteine substitutions affected functional properties of the proteins, each mutant was assayed for ATPase and chaperone activity as well as for interactions with peptides and IscU. Table I shows the ATPase activity of wild-type HscA, HscA(Q421C), HscA(D422C), and HscA(A455C) in the absence and presence of the different peptides and forms of IscU. The parent HscA(C315S/C448S) mutant displayed an elevated basal ATPase activity compared with wild-type HscA (0.46 *versus* 0.10 min^{-1}), and a similar increase was observed for the three site-specific cysteine mutants (0.37–0.80 min^{-1}). Each of the mutants exhibited peptide and IscU-stimulated ATPase activity indicating retention of allosteric coupling of ATPase activity with substrate binding. Synergistic stimulation by IscU in the presence of HscB (8) was also observed indicating that the coupling between substrate and co-chaperone activation was not altered. The effects of the cysteine substitutions on the affinity for IscU were further

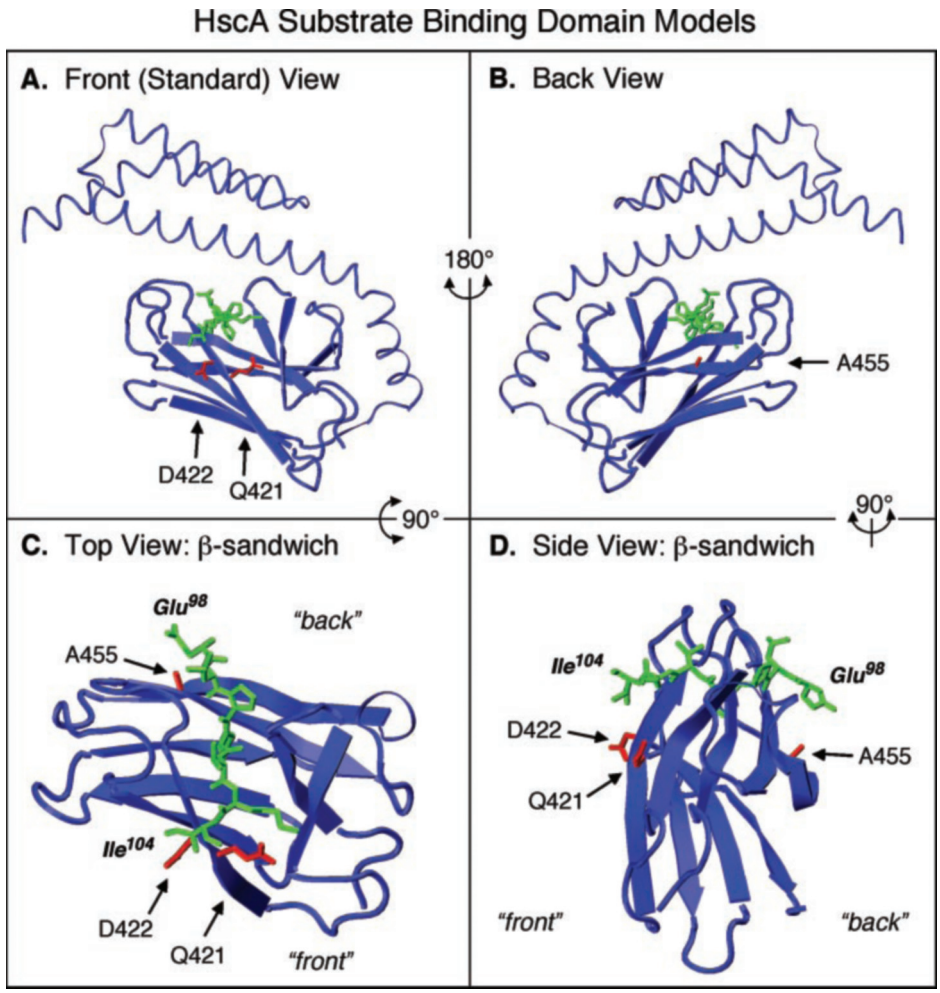

FIG. 2. **Model of the HscA substrate binding domain with bound peptide.** *Panels A* and *B* include residues 391–606 with the view shown in *panel A* corresponding to the standard view of DnaK from Ref. 14. *Panels C* and *D* include only residues 391–500 of the β-sandwich subdomain. Rotations used to generate different views are indicated. The peptide backbone of HscA is shown in *blue*, and a peptide corresponding to residues 98–104 of IscU (ELPPVKI) is shown in *green*. Side chains of HscA residues selected for cysteine mutagenesis and bimane labeling are shown in *red*. The model shown, with the peptide in the reverse orientation from that observed for the DnaK-NRLLLTG complex, is derived from Ref. 13. The structural representations were generated using VMD (39).

TABLE I

Stimulation of ATPase activity of HscA cysteine mutants by peptides and IscU mutants

Reactions were carried out with 5 μM HscA at 25 °C in HKM buffer. Basal activities were determined in the absence of added peptide or IscU. Additions: peptides, 300 μM; IscU, IscU(L97W) and IscU(H105W), 100 μM; HscB, 50 μM. The concentrations used are near saturating levels (*cf.* Figs. 4 and 7), and the specific activities reported (mole of ATP hydrolyzed/mol of HscA/min) therefore reflect approximate maximal turnover numbers.

	ATP hydrolysis							
	Basal	+Glu^{98}–Cys^{106}	+W-97	+W-105	+IscU	+L97W	+H105W	+IscU + HscB
				min^{-1}				
HscA	0.10	0.29	0.36	0.30	0.70	0.55	0.36	49.8
HscA(Q421C)	0.44	0.74	1.58	0.94	1.16	1.50	0.79	44.7
HscA(D422C)	0.80	1.02	1.23	1.04	2.10	1.87	1.27	42.8
HscA(A455C)	0.37	0.73	0.94	0.72	1.64	1.24	0.67	64.1

assessed by isothermal titration calorimetry, and each of the mutants bound IscU with an affinity comparable with that of wild-type HscA: HscA K_d = 3.0 μM, HscA(Q421C) K_d = 2.9 μM, HscA(D422C) K_d = 1.0 μM, and HscA(A455C) K_d = 9.4 μM. All mutants also displayed chaperone activity similar to that of wild-type HscA (20) as assessed by suppression of aggregation of the model substrate rhodanese (data not shown). Taken together, these results suggest that HscA(Q421C), HscA(422C), and HscA(455C) represent active HscA mutants without major alterations in their functional properties.

Peptide Quenching of Bimane-labeled HscA—The HscA cysteine mutants were labeled with bimane, and initial studies on their interactions with peptides were carried out in the absence of nucleotides. Fig. 3 shows the effects of the wild-type Glu^{98}–Cys^{108} peptide and the tryptophan containing W-97 and W-105 peptides on the bimane fluorescence emission of both front- and back-labeled HscA. For the front-labeled HscA(D422C)-bimane derivative the Glu^{98}–Cys^{106} and W-97 peptides gave only weak quenching (≅6%), whereas the W-105 peptide quenched bimane fluorescence ≅21%. The enhanced quenching by W-105 relative to W-97 suggests that the bound peptide is preferentially oriented with the C terminus on the front face of the substrate binding domain proximal to residue 422 (see Fig. 2). The difference in quenching efficiency of W-97 and W-105 indicates that >90% of the peptide is bound in this reverse (back to front) orientation.

The effects of the peptides on the fluorescence of the back-labeled HscA(A455C)-bimane mutant were also consistent with preferential binding orientation. For this derivative there was substantial quenching (≅29%) of bimane fluorescence by the Glu^{98}–Cys^{108} peptide, suggesting that peptide binding itself alters the emission efficiency of the probe at position 455. However, a large difference in quenching efficiency was observed with the tryptophan-labeled peptides. The W-105 peptide produced only

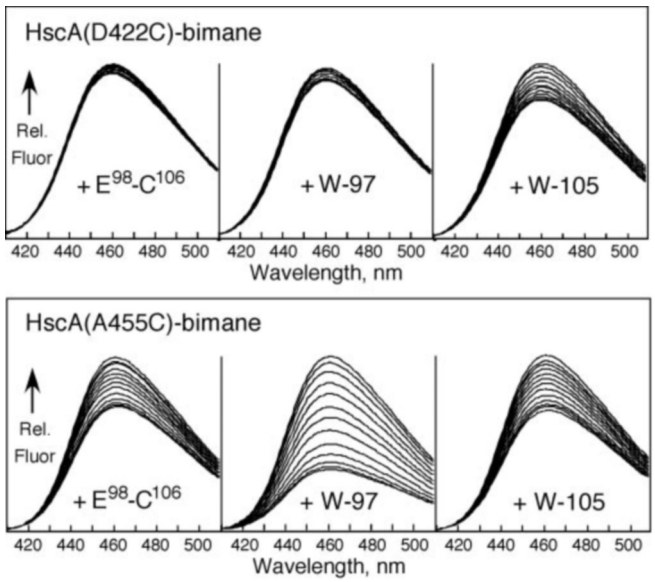

FIG. 3. **Effects of tryptophan peptides on the fluorescence of bimane-labeled HscA.** Emission spectra of bimane-labeled HscA(D422C) and HscA(A455C) in HKM buffer, 25 °C, were recorded following successive additions of Glu^{98}–Cys^{106}, W-97, or W-105 (0.9- 274 μM final concentrations); the uppermost spectrum for each sample was recorded prior to addition of peptide.

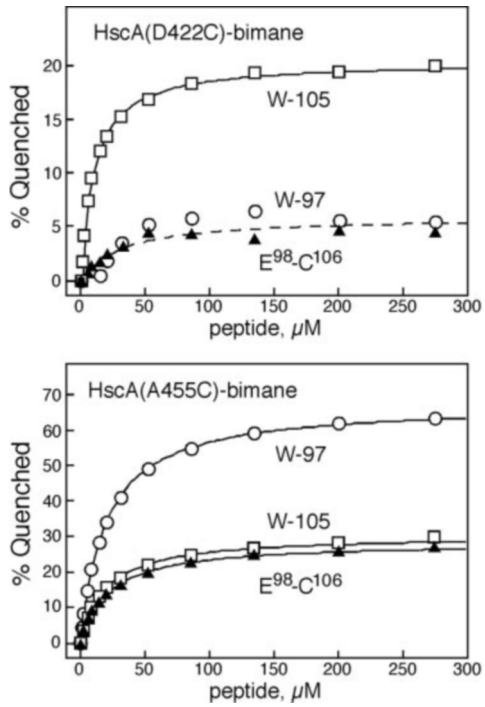

FIG. 4. **Binding of peptides to bimane-labeled HscA monitored by fluorescence quenching.** Fractional quenching values determined from the integrated emission intensities in Fig. 3 were fit to hyperbolic saturation functions to determine K_d and maximal quenching. HscA(D422C)-bimane: data for +Glu^{98}–Cys^{106} (▲) and +W-97 (○) were not fit, and the *dashed curve* shown was generated using K_d = 30 μM (max = 6%); +W-105 (□) K_d = 9.8 μM (max = 20.5%). HscA(A455C)-bimane: +Glu^{98}–Cys^{106} (▲) K_d = 21.4 μM (max = 29%), +W-97 (○) K_d = 19.1 μM (max = 68%), +W-105 (□, *open squares*) K_d = 19.2 μM (max = 31%).

marginally greater quenching than Glu^{98}–Cys^{106} (31 *versus* 29%), whereas the W-97 peptide was much more effective (≅68%). These results indicate a strong preference (>10:1) for peptide binding in which the N terminus is located on the back side of the substrate binding domain, *i.e.* the same reverse orientation as observed with the HscA(D422C)-bimane derivative. Whereas it is possible that the failure of specific peptides to quench fluorescence could result from restricted positioning of the tryptophan residue, the agreement of the findings with front- and back-labeled HscA-bimane derivatives argues in favor of a single preferred orientation.

The binding affinity of the peptides for the HscA-bimane derivatives was analyzed by integration of the emission curves in Fig. 3 at each concentration of added peptide (Fig. 4). For bimane-labeled HscA(D422C) the extent of quenching by Glu^{98}–Cys^{106} and W-97 was too low to analyze with confidence, but the data show an approximate fit to a binding curve corresponding to K_d ~30 μM. Data for the W-105 peptide fit a curve corresponding to K_d ≅10 μM. For bimane-labeled HscA(A455C) each of the peptides displayed a normal saturation curve and bound with similar affinity, K_d ≅ 20 μM. The similarities of the affinities of the W-97 and W-105 peptides to that of Glu^{98}–Cys^{106} suggest that the presence of tryptophan at the N or C terminus does not dramatically alter binding interactions. The lack of a major effect of the terminal tryptophan residues on binding affinity is consistent with the HscA-peptide model in which residues 97 and 105 are positioned outside of the immediate peptide binding cleft (see Fig. 2).

Similar fluorescence quenching experiments were carried out using the HscA(Q421C)-bimane derivative (see Supplemental Materials Fig. 1). As with HscA(D422C)-bimane the Glu^{98}–Cys^{106} and W-97 peptides had weaker effects (maximal quenching <16%) than the W-105 peptide (≅38% maximal quenching). The finding that similar results are obtained using a different front side labeling position provide additional support for the preferential back to front binding orientation.

Nucleotide Effects on Peptide Binding—The affinity of hsp70s for substrates is nucleotide-dependent (26–33), and nucleotide-free and ADP-bound (R-state) forms of HscA exhibit high substrate affinity relative to the ATP-bound (T-state) form (8, 9, 20). To determine whether the bimane-labeled HscA mutants retain this allosteric coupling we monitored peptide-induced quenching in the presence of ADP or ATP. As shown in Fig. 5 binding of W-105 to bimane-labeled HscA(D422C) and W-97 to bimane-labeled HscA(A455C) is nucleotide-dependent. The affinity of HscA(D422C)-bimane for W-105 is ≅17-fold lower in the presence of ATP than in the presence of ADP, and the affinity of HscA(A455C)-bimane for W-97 is reduced ≅6-fold in the presence of ATP compared with the ADP-bound state. In both cases the affinities observed in the presence of ADP are similar to those observed in the absence of nucleotide (compare Fig. 4). These results indicate that neither the mutations introduced in HscA(C315S, C448S, and D422C, or A455C) nor the presence of the bimane probe impair interdomain communication.

Quenching by IscU Mutants—To determine whether the preferential binding orientation observed with the W-97 and W-105 peptides occurred with the full-length IscU protein we prepared the corresponding IscU(L97W) and IscU(H105W) mutant proteins. Both mutants exhibited chromatographic behavior similar to wild-type IscU during purification (data not shown), suggesting that introduction of tryptophan at these positions did not grossly affect the structure of the protein; subsequent size exclusion chromatography revealed that wild-type IscU and IscU(H105W) behaved as dimers, whereas IscU(97W) exhibited chromatographic behavior indicative of a tetramer. Both mutants were active in stimulating the ATPase activity of wild-type HscA as well as each of the cysteine mutants (Table I) consistent with their interaction with the substrate binding domain in a manner similar to wild-type IscU.

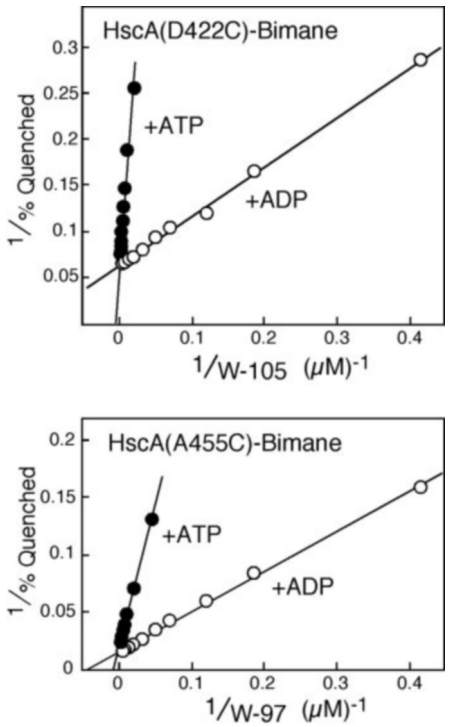

FIG. 5. **Effects of ADP and ATP on binding of tryptophan peptides to bimane-labeled HscA.** Fluorescence emission spectra of bimane-labeled HscA in the presence of nucleotide were measured following addition of peptide (1 mM ADP + 2.4–270 μM peptide; 5 mM ATP + 50–900 μM peptide). Integrated emission intensities were plotted and fit by linear regression. HscA(D422C)-bimane + W-105: K_d (+ADP) = 8.5 μM, K_d (+ATP) = 148 μM. HscA(A455C)-bimane + W-97: K_d (+ADP) = 21.6 μM, K_d (+ATP) = 122 μM.

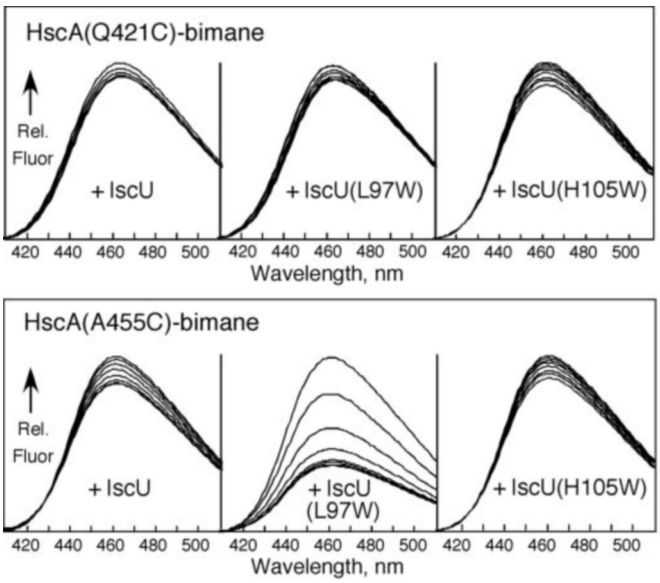

FIG. 6. **Effects of IscU tryptophan mutants on the fluorescence of bimane-labeled HscA.** Emission spectra of bimane-labeled HscA(Q421C) and HscA(A455C) in HKM buffer, 25 °C, were recorded following addition of IscU, IscU(L97W), or IscU(H105W) (2.5–56.6 μM final concentrations); the *uppermost spectrum* for each sample is prior to addition of IscU.

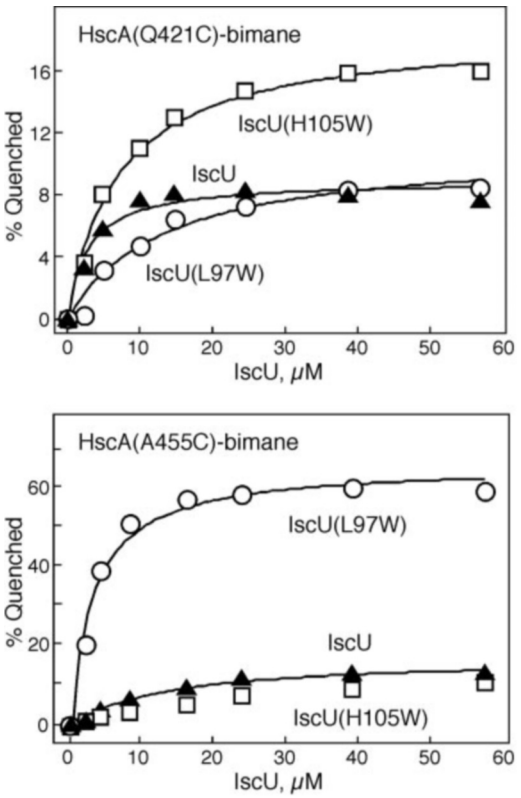

FIG. 7. **Binding of IscU tryptophan mutants to bimane-labeled HscA monitored by fluorescence quenching.** Fractional quenching values determined from the integrated emission intensities in Fig. 6 were fit to hyperbolic saturation functions to determine K_d and maximal quenching. HscA(Q421C)-bimane: +IscU (▲) K_d = 2.8 μM, max = 9.1%; +IscU(L97W) (○) K_d = 13.0 μM (max = 11.1%); IscU(H105W) (□) K_d = 7.0 μM, (max = 18.7%). HscA(A455C)-bimane: +IscU (▲) K_d = 12.6 μM (max = 17.3%); +IscU(L97W) (○) K_d = 3.0 μM (max = 65.7%); IscU(H105W) (□) was not fit.

Fluorescence experiments carried out using bimane-labeled HscA(D422C) showed weak effects of IscU(L97W) and IscU(H105W) on the fluorescence of this derivative (see Supplemental Materials Fig. 2). Addition of IscU(H105W) led to a small degree of quenching (≅7%), whereas the IscU(L97W) mutant gave a small increase in fluorescence (≅8%). The fact that quenching is observed only with IscU(H105W) is consistent with the reverse orientation deduced from the peptide binding experiments described above. However, the small effects observed make it difficult to determine binding affinities and to interpret the results using this derivative with confidence. The structure of the IscU protein may restrict access of tryptophan to the bimane label in this complex, and conformational changes induced in HscA by IscU binding could affect fluorescence yields of the label.

Fluorescence quenching studies using the HscA(Q421C) mutant were more straightforward. The effects of wild-type IscU, IscU(L97W), and IscU(H105W) on the fluorescence emission of front-labeled HscA(Q421C) and back-labeled HscA(A455C) derivatives are shown in Fig. 6. The results are similar to those found for the corresponding peptides shown in Fig. 3. For HscA(Q421C)-bimane wild-type IscU and IscU(L97W) caused weak quenching (≅8%), whereas IscU(H105W) caused ≅16% quenching. For HscA(A455C)-bimane, on the other hand, IscU(H105W) was no more effective than wild-type IscU (≅12%), whereas IscU(L97W) caused ≅60% quenching. These results indicate that, as found for the peptides, the IscU protein exhibits a strong (>10:1) preference for binding in which the N terminus is located on the back side and the C terminus is located on the front side of the substrate binding domain, *i.e.* the reverse (back to front) orientation. The similarity in directional binding preference for the full-length IscU protein to that observed for the isolated peptides further suggests that the positively charged N-terminal amine and/or the negatively charged C-terminal carboxyl of the peptides do not contribute significantly to binding polarity.

Analyses of the binding affinities of IscU, IscU(L97W), and IscU(H105W) for the bimane-labeled HscA mutants are shown in Fig. 7. The K_d values observed for wild-type IscU are similar to those found by isothermal titration calorimetry for binding to the unlabeled HscA mutants (see above) indicating that bimane labeling itself does not significantly interfere with binding. For HscA(Q421C)-bimane both IscU(L97W) and IscU(H105W) exhibited slightly reduced affinity relative to wild-type IscU (4- and 2-fold, respectively), suggesting that the tryptophan substitutions have a small effect on the interaction with this labeled derivative. For HscA(A455C)-bimane the affinity of IscU(H105W) could not be determined accurately because of the low extent of quenching; binding of IscU(L97W), however, occurred with slightly higher affinity than wild-type IscU. Whereas small differences in affinities are apparent, the overall results are consistent with IscU(L97W) and IscU(H105W) binding to bimane-labeled HscA in a similar manner as wild-type IscU.

HscB Effects on IscU Binding Orientation—Interaction of IscU with the ATP complex of HscA (T-state) is facilitated by the J-type co-chaperone HscB (8). To determine whether HscB affects the orientation of IscU when bound to HscA(ATP) we carried out fluorescence quenching studies in the presence of the co-chaperone. HscB alone had no effect on the fluorescence of the HscA(A455C)-bimane-ATP complex. In the case of the HscA(Q421C)-bimane-ATP complex, however, HscB binding resulted in an increase in fluorescence intensity (≅22%) accompanied by a blue shift (≅3 nm) in the emission maximum (data not shown); these changes are presumed to result from changes in the environment of the bimane probe resulting from HscB binding.

Because IscU and HscB synergistically stimulate the ATPase activity of HscA (8), it was not possible to carry out complete titrations as with IscU alone because of the enhanced hydrolysis and depletion of ATP. Instead, fluorescence spectra were recorded before and immediately following addition of a saturating mixture of HscB plus IscU to HscA in the presence of excess ATP. As shown in Fig. 8, addition of wild-type IscU with HscB to the HscA(Q421C)-bimane-ATP complex caused a small increase in fluorescence intensity (≅12%) and shift in emission maximum (470 to 467 nm). The increase observed is less than that following addition of HscB alone (see above), suggesting that IscU binding results in slight quenching of this derivative as was observed in the absence of HscB (Figs. 6 and 7). Addition of IscU(L97W) with HscB to HscA(Q421C)-bimane caused a similar fluorescence change to that observed with wild-type IscU consistent with the positioning of residue 97 on the side opposite to the bimane label, *i.e.* on the back side of the HscA substrate binding domain. Addition of IscU(H105W) with HscB, in contrast, resulted in ≅30% quenching suggesting that, as in the absence of HscB, residue 105 is positioned on the front face of the substrate binding domain in the HscA(ATP)-IscU-HscB complex.

Results with HscA(A455C)-bimane also indicate a reverse (back to front) orientation for IscU complexed to HscA in the presence of HscB. Wild-type IscU and IscU(H105W) with HscB caused ≅11% quenching for this derivative, a value similar to that observed in the absence of HscB (8–11%; Figs. 6 and 7) and consistent with positioning of C-terminal residues of IscU on the front side of the HscA substrate binding domain. Addition of IscU(L97W) with HscB, on the other hand, resulted in ≅46% quenching consistent with positioning of the N-terminal residues of IscU on the back side of the substrate binding domain. These results, together with those for the HscA(Q421C)-bimane-ATP complex, indicate that interaction of HscB with IscU and HscA(ATP) does not affect the orientation of the IscU recognition sequence in the peptide binding cleft.

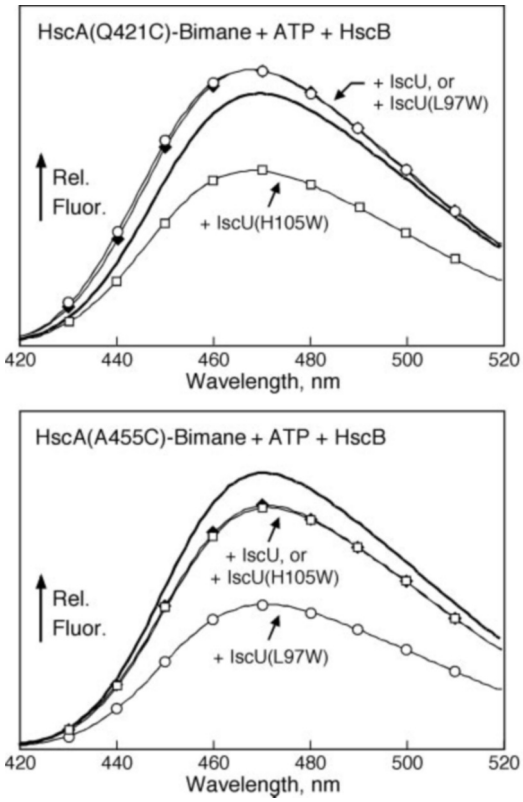

FIG. 8. **Effects of HscB on IscU-mediated quenching of bimane-labeled HscA fluorescence.** Emission spectra of bimane-labeled HscA(Q421C) and HscA(A455C) in the presence of 5 mM ATP were recorded before (*heavy line*) and following addition of IscU (▲) IscU(L97W) (○), or IscU(H105W) (□) with HscB. IscU and HscB were pre-equilibrated at a 1:1 ratio and added to give a final concentration (56 μM) sufficient to saturate binding to HscA.

DISCUSSION

The studies presented herein reveal that HscA displays a strong directional preference for binding of IscU- and IscU-derived peptides containing the LPPVK recognition motif. Whereas the bimane fluorescent probe employed exhibits some sensitivity to environmental effects, comparison of the extent of quenching of HscA labeled on opposite sides of the substrate binding domain by N- and C-terminal tryptophan containing peptides establishes that the reverse (back to front) binding orientation is greater than 10-fold more favorable than the forward (front to back) orientation. The finding that short peptides containing the LPPVK sequence were bound with the same polarity as the IscU protein and the lack of an effect of the co-chaperone HscB on binding orientation further indicate that interactions involving the LPPVK region with the substrate binding domain are major contributors to binding orientation. These results are consistent with our previously proposed models in which the LPPVK region binds to the substrate binding domain in an extended conformation with Pro^{101} centrally positioned in the peptide binding cleft (13).

Implications for Iron-Sulfur Cluster Assembly—IscU has been proposed to serve as a scaffold for the transient assembly of iron-sulfur clusters (10, 11), and the interaction of HscA and IscU may play an important role in iron-sulfur cluster formation and/or transfer. The binding orientation that we observe places significant restrictions on the positioning of different regions of the IscU polypeptide relative to the chaperone. Amino acids of IscU that are N-terminal to the LPPVK motif (residues 2–98) will be positioned on the back side of the HscA

substrate binding domain, whereas those C-terminal (residues 104–128) will be positioned on the front side (see Fig. 2). Assuming that the structure of the HscA substrate binding domain is similar to that of DnaK (Ref. 14, see also Ref. 13), the size of the β-sandwich subdomain comprising the binding cleft and the α-helical subdomain comprising the lid appear likely to prevent intramolecular interactions between the N- and C-terminal regions of IscU. This may have important functional consequences for iron-sulfur cluster formation. The structure of the iron-sulfur complex of IscU is not known, but cysteine residues have been implicated in cluster coordination (10, 11, 34–36). In the HscA-IscU complex residues Cys^{37} and Cys^{63} of IscU are positioned on the back side of the HscA substrate binding domain, whereas Cys^{106} is restricted to the front side. This spatial separation will ostensibly prevent Cys^{106} from interacting with the same iron-sulfur cluster as Cys^{37} and Cys^{63} while bound to HscA. However, interactions of Cys^{106} with Cys^{37} and/or Cys^{63} from another IscU subunit could occur, and biochemical studies indicate that IscU iron-sulfur complexes exist as a dimer or higher oligomer (8, 10, 11, 34–36) that could allow for intersubunit cluster binding.

The effects of HscA binding on the structure of IscU are not known. NMR studies of apo-IscU from *Thermotoga maritima* indicate that this protein exhibits a limited tertiary structure in solution and that the region including residues corresponding to the LPPVK motif and Cys^{106} of *E. coli* IscU is intrinsically unstructured (37, 38). In contrast, unpublished NMR studies of IscU from *Haemophilus influenzae* show that the apo-form of this IscU protein is folded in solution.[2] In *H. influenzae* IscU Cys^{106} is positioned close to Cys^{37} and Cys^{63}, and the LPPVK region is located nearby as a loop connecting the secondary structure elements. Based on this structure it would appear that binding of *H. influenzae* IscU to HscA would require significant disruption of the tertiary structure of the IscU protein. Further studies on the effects of HscA on the IscU structure and iron-sulfur cluster formation may provide insight into the role of the chaperone in cluster formation and/or transfer.

Comparison with Other hsp70 Peptide Complexes—The back to front orientation of IscU- and IscU-derived peptides relative to the substrate binding domain of HscA is opposite that described previously for other hsp70 peptide complexes. The original crystal structure of the substrate binding domain of *E. coli* DnaK showed that the synthetic peptide NRLLLTG was bound with its N terminus facing the side containing residues homologous to HscA residues 421 and 422 and its C terminus facing the side containing the residue homologous to HscA residue 455 (14), we have designated this as the forward direction. The central leucine residue of the NRLLLTG peptide was bound in a hydrophobic pocket in the center of the cleft with adjacent leucine residues flanking the arch (formed by Met^{404} and Ala^{429}) over the pocket (14). Subsequent solution NMR studies of a complex of the NRLLLTG peptide and a truncated form of the DnaK substrate binding domain containing only the β-sandwich subdomain (residues 393–507) showed binding in the same register and forward orientation as was observed in the crystal structure (40). NMR studies on other forms of DnaK and Hsc70 have also revealed intramolecular "pseudo-substrate" types of binding interactions. Studies employing a truncated DnaK substrate binding domain fragment (residues 386–561) showed that a portion of the C-terminal helical subdomain was unwound in solution and was bound to the peptide binding cleft of the β-sandwich subdomain (41). As found with the DnaK-NRLLLTG complexes, the DnaK peptide segment was positioned in a forward direction with Leu^{543} bound in the central pocket and Leu^{542} and His^{544} on the front and back sides, respectively, of the arch (41). Similar results were also obtained in solution NMR studies of a truncated fragment of rat Hsc70 (residues 383–540). The C terminus of Hsc70 was unfolded, and Leu^{549} was bound in the central pocket with Ser^{538} and Glu^{540} located adjacent to the arch in positions corresponding to the forward direction (42).

What Determines Peptide Binding Orientation?—For the hsp70s studied to date, DnaK, Hsc70, and HscA, peptide binding appears to occur with a preferred orientation. It is not known, however, whether specific directional binding is unique to these protein-peptide complexes or is a general feature of hsp70 chaperones. It is also not known whether the forward binding orientation observed with DnaK and Hsc70 or the reverse orientation observed with HscA occurs most commonly. Examination of the crystal structure of the DnaK-NRLLLTG complex suggests that selectivity for residue type is greatest at the central site "0" in which a deep hydrophobic pocket would appear to favor large aliphatic side chains (14), and this feature could be important in determining the register of binding. The factors that influence the peptide orientation, however, are less clear. The NRLLLTG peptide is involved in a number of main chain hydrogen bonds and van der Waals interactions that could be important in determining binding polarity, but small structural rearrangements might allow binding in the reverse direction with similarly favorable interactions. Studies of the interaction of DnaK with cellulose-bound peptides (45) have shown that peptides having an inverse sequence appear to differ somewhat in binding affinity, suggesting that stereochemical constraints on both peptide backbone and side chain interactions may contribute to both binding specificity and directionality.

Electrostatic factors may also influence binding. The region surrounding the peptide binding cleft of DnaK has a negative potential that favors peptides containing basic residues (14, 43, 44). However, this potential is most pronounced on the C-terminal side of the cleft, and the NRLLLTG peptide is bound with its basic N terminus on the less negative side and the acidic C terminus on the more negative side (14). This suggests that for this peptide complex of DnaK the electrostatic potential plays a lesser role in determining binding polarity. Studies on the effects of ionic strength on binding of the NRLLLTG peptide to DnaK have indicated an electrostatic free energy of binding about −1 kcal/mol (46), but empirical calculations based on binding of several charge derivatives to DnaK suggest that nonpolar interactions are the predominant contributor to the free energy of binding (47).

The relative importance of steric factors, specific bonding interactions, and electrostatic potential may vary for different hsp70s. In the case of HscA-IscU interactions the preference for proline at the central position of the peptide will impose geometric restrictions because of the shape and rigidity of the pyrrolidine ring. In addition, the presence of an imine nitrogen in the peptide backbone at this position will preclude the type of hydrogen bonding observed with the NRLLLTG complex with DnaK. Models of the substrate binding domain of HscA also suggest an asymmetric charge distribution with acidic residues near the front side of the cleft and basic residues near the back side (13), and these could contribute significantly to binding energy. Indeed, modeling studies suggested the possibility that the reverse peptide binding orientation observed here might allow Glu^{98} and Lys^{103} of IscU to participate in specific charge interactions with HscA and favor that orientation (see Ref. 13, Fig. 9). Determination of the structure of additional hsp70-peptide complexes, especially those like the

[2] T. A. Ramelot, J. R. Cort, G. T. Montelione, and M. A. Kennedy, Protein Data Bank Code 1Q48, Research Collaboratory for Structural Bioinformatics, Rutgers University, New Brunswick, NJ (http://www.rcsb.org/).

HscA-IscU complex in which peptide is bound in the reverse direction from that of the DnaK-NRLLLTG complex, would improve our understanding of factors determining substrate selectivity by this class of molecular chaperone.

Acknowledgments—We thank Dennis Ta and Kristi Fox for expert technical assistance, Alexey Ladokhin for advice and assistance with fluorescence measurements, and Jonathon Silberg for helpful discussions.

REFERENCES

1. Seaton, B. L., and Vickery, L. E. (1994) *Proc. Natl. Acad. Sci. U. S. A.* **91,** 2066–2070
2. Kawula, T. H., and Lelivelt, M. J. (1994) *J. Bacteriol.* **176,** 610–619
3. Vickery, L. E., Silberg, J. J., and Ta, D. T. (1997) *Protein Sci.* **6,** 1047–1056
4. Strain, J., Lorenz, C. R., Bode, J., Garland, S., Smolen, G. A., Ta, D. T., Vickery, L. E., and Culotta, V. C. (1998) *J. Biol. Chem.* **273,** 31138–31144
5. Zheng, L., Cash, V. L., Flint, D. H., and Dean, D. R. (1998) *J. Biol. Chem.* **273,** 13264–13272
6. Takahashi, Y., and Nakamura, M. (1999) *J. Biochem.* (*Tokyo*) **126,** 917–926
7. Tokumoto, U., and Takahashi, Y. (2001) *J. Biochem.* (*Tokyo*) **130,** 63–71
8. Hoff, K. G., Silberg, J. J., and Vickery, L. E. (2000) *Proc. Natl. Acad. Sci. U. S. A.* **97,** 7790–7795
9. Silberg, J. J., Hoff, K. G., Tapley, T. L., and Vickery, L. E. (2001) *J. Biol. Chem.* **276,** 1696–1700
10. Agar, J. N., Krebs, C., Frazzon, J., Huynh, B. H., Dean, D. R., and Johnson, M. K. (2000) *Biochemistry* **39,** 7856–7862
11. Agar, J. N., Zheng, L., Cash, V. C., Dean, D. R., and Johnson, M. K. (2000) *J. Am. Chem. Soc.* **122,** 2136–2137
12. Hoff, K. G., Ta, D. T., Tapley, T. L., Silberg, J. J., and Vickery, L. E. (2002) *J. Biol. Chem.* **277,** 27353–27359
13. Hoff, K. G., Cupp-Vickery, J., and Vickery, L. E. (2003) *J. Biol. Chem.* **278,** 37582–37589
14. Zhu, X., Zhao, X., Burkholder, W. F., Gragerov, A., Ogata, C. M., Gottesman, M. E., and Hendrickson, W. A. (1996) *Science* **272,** 1606–1614
15. Riddles, P. W., Blakeley, R. L., and Zerner, B. (1979) *Anal. Biochem.* **94,** 75–81
16. Gill, S. C., and von Hippel, P. H. (1989) *Anal. Biochem.* **182,** 319–326
17. Mach, H., Middaugh, C. R., and Lewis, R. V. (1992) *Anal. Biochem.* **200,** 74–80
18. Pace, C. N., Vajdos, F., Fee, L., Grimsley, G., and Gray, T. (1995) *Protein Sci.* **4,** 2411–2423
19. Mansoor, S. E., Mchaourab, H. S., and Farrens, D. L. (1999) *Biochemsitry* **38,** 16383–16393
20. Silberg, J. J., Hoff, K. G., and Vickery, L. E. (1998) *J. Bacteriol.* **180,** 6617–6624
21. Silberg, J. J., and Vickery, L. E. (2000) *J. Biol. Chem.* **275,** 7779–7786
22. Sato, E., Sakashita, M., Kanaoka, Y., and Kosower, E. M. (1988) *Bioorg. Chem.* **16,** 298–306
23. Kosower, E. M., and Kosower, N. S. (1995) *Methods Enzymol.* **251,** 133–148
24. Kosower, E. M., Giniger, R., Radkowsky, A., Hebel, D., and Shusterman, A. (1986) *J. Phys. Chem.* **90,** 5552–5557
25. Mansoor, S. E., McHaourab, H. S., and Farrens, D. L. (2002) *Biochemistry* **41,** 2475–2484
26. Beckmann, R. P., Mizzen, L. E., and Welch, W. J. (1990) *Science* **248,** 850–854
27. Palleros, D. R., Welch, W. J., and Fink, A. L. (1991) *Proc. Natl. Acad. Sci. U. S. A.* **88,** 5719–5723
28. Palleros, D. R., Reid, K. L., Shi, L., Welch, W. J., and Fink, A. L. (1993) *Nature* **365,** 664–666
29. Schmid, D., Baici, A., Gehring, H., and Christen, P. (1994) *Science* **263,** 971–973
30. McCarty, J. S., Buchberger, A., Reinstein, J., and Bukau, B. (1995) *J. Mol. Biol.* **249,** 126–137
31. Greene, L. E., Zinner, R., Naficy, S., and Eisenberg, E. (1995) *J. Biol. Chem.* **270,** 2967–2973
32. Takeda, S., and McKay, D. B. (1996) *Biochemistry* **35,** 4636–4644
33. Theyssen, H., Schuster, H. P., Packschies, L., Bukau, B., and Reinstein, J. (1996) *J. Mol. Biol.* **263,** 657–670
34. Foster, M. W., Mansy, S. S., Hwang, J., Penner-Hahn, J. E., Surerus, K. K., and Cowan, J. A. (2000) *J. Am. Chem. Soc.* **122,** 6805–6806
35. Mansy, S. S., Wu, G., Surerus, K. K., and Cowan, J. A. (2002) *J. Biol. Chem.* **277,** 21397–21404
36. Wu, G., Mansy, S. S., Wu, S. P., Surerus, K. K., Foster, M. W., and Cowan, J. A. (2002) *Biochemistry* **41,** 5024–5032
37. Bertini, I., Cowan, J. A., Del Bianco, C., Luchinat, C., and Mansy, S. S. (2003) *J. Mol. Biol.* **331,** 907–924
38. Mansy, S. S., Wu, S.-P., and Cowan, J. A. (2004) *J. Biol. Chem.* **279,** 10469–10475
39. Humphrey, W., Dalke, A., and Shulten, K. (1996) *J. Mol. Graph.* **14,** 33–38
40. Stevens, S. Y., Cai, S., Pellecchia, M., and Zuiderweg, E. R. (2003) *Protein Sci.* **12,** 2588–2596
41. Wang, H., Kurochkin, A. V., Pang, Y., Hu, W., Flynn, G. C., and Zuiderweg, E. R. (1998) *Biochemistry* **37,** 7929–7940
42. Morshauser, R. C., Hu, W., Wang, H., Pang, Y., Flynn, G. C., and Zuiderweg, E. R. (1999) *J. Mol. Biol.* **289,** 1387–1403
43. Rudiger, S., Germeroth, L., Schneider-Mergener, J., and Bukau, B. (1997) *EMBO J.* **16,** 1501–1507
44. Rudiger, S., Buchberger, A., and Bukau, B. (1997) *Nat. Struct. Biol.* **4,** 342–348
45. Rudiger, S. Schneider-Mergener, J., and Bukau, B. (2001) *EMBO J.* **20,** 1042–1050
46. Liu, W., Bratko, D., Prausnitz, J. M., and Blanch, H. W. (2003) *J. Phys. Chem.* **107,** 11563–11569
47. Kasper, P., Christen, P., and Gehring, H. (2000) *Proteins Struct. Funct. Genet.* **40,** 185–192